Gastroenterology 2020;159:2181–2192

Clostridioides difficile Toxin A Remodels Membranes and Mediates DNA Entry Into Cells to Activate Toll-Like Receptor 9 Signaling

Xinhua Chen,[1,*] **Xiaotong Yang**,[1,2,*] **Jaime de Anda**,[3,*] Jun Huang,[1,4] Dan Li,[1] Hua Xu,[1] Kelsey S. Shields,[1] Mária Džunková,[5] Joshua Hansen,[1] Ishan J. Patel,[6] Eric U. Yee,[7] Douglas T. Golenbock,[8] Marianne A. Grant,[9] Gerard C. L. Wong,[3] and Ciarán P. Kelly[1]

[1]*Division of Gastroenterology, Beth Israel Deaconess Medical Center, Harvard Medical School, Boston, Massachusetts;* [2]*Institute of Microbiology and Immunology, College of Life Sciences, Shanghai Normal University, Shanghai, China;* [3]*Department of Bioengineering, Department of Chemistry and Biochemistry, California Nano Systems Institute, University of California, Los Angeles, Los Angeles, California;* [4]*Department of Colorectal Surgery, The 6th Affiliated Hospital, Sun Yat-sen University, Guangzhou, China;* [5]*US Department of Energy Joint Genome Institute, Lawrence Berkeley National Laboratory, Berkeley, California;* [6]*Stony Brook University Hospital, Stony Brook, New York;* [7]*Department of Pathology, University of Arkansas for Medical Sciences, Little Rock, Arkansas;* [8]*Division of Infectious Diseases and Immunology, University of Massachusetts Medical School, Worcester, Massachusetts; and* [9]*Division of Molecular and Vascular Medicine, Department of Medicine, Beth Israel Deaconess Medical Center, Harvard Medical School, Boston, Massachusetts*

BACKGROUND & AIMS: *Clostridioides difficile* toxin A (TcdA) activates the innate immune response. TcdA co-purifies with DNA. Toll-like receptor 9 (TLR9) recognizes bacterial DNA to initiate inflammation. We investigated whether DNA bound to TcdA activates an inflammatory response in murine models of *C difficile* infection via activation of TLR9. **METHODS:** We performed studies with human colonocytes and monocytes and macrophages from wild-type and TLR9 knockout mice incubated with TcdA or its antagonist (ODN TTAGGG) or transduced with vectors encoding TLR9 or small-interfering RNAs. Cytokine production was measured with enzyme-linked immunosorbent assay. We studied a transduction domain of TcdA ($TcdA_{57–80}$), which was predicted by machine learning to have cell-penetrating activity and confirmed by synchrotron small-angle X-ray scattering. Intestines of CD1 mice, C57BL6J mice, and mice that express a form of TLR9 that is not activated by CpG DNA were injected with TcdA, TLR9 antagonist, or both. Enterotoxicity was estimated based on loop weight to length ratios. A TLR9 antagonist was tested in mice infected with *C difficile*. We incubated human colon explants with an antagonist of TLR9 and measured TcdA-induced production of cytokines. **RESULTS:** The $TcdA_{57–80}$ protein transduction domain had membrane remodeling activity that allowed TcdA to enter endosomes. TcdA-bound DNA entered human colonocytes. TLR9 was required for production of cytokines by cultured cells and in human colon explants incubated with TcdA. TLR9 was required in TcdA-induced mice intestinal secretions and in the survival of mice infected by *C difficile*. Even in a protease-rich environment, in which only fragments of TcdA exist, the $TcdA_{57–80}$ domain organized DNA into a geometrically ordered structure that activated TLR9. **CONCLUSIONS:** TcdA from *C difficile* can bind and organize bacterial DNA to activate TLR9. TcdA and TcdA fragments remodel membranes, which allows them to access endosomes and present bacterial DNA to and activate TLR9. Rather than inactivating the ability of DNA to bind TLR9, TcdA appears to chaperone and organize DNA into an inflammatory, spatially periodic structure.

Keywords: SAXS; Antibiotic-Associated Diarrhea and Colitis; Intestinal Inflammation; Pore Formation.

Clostridioides (formerly *Clostridium*) *difficile* is an important pathogen of worldwide distribution and a frequent cause of death from severe colitis.[1–3] The incidence and severity of *C difficile* infection (CDI) have increased dramatically in Europe and North America in recent years.[1] The major virulence factors of *C difficile* are 2 large protein exotoxins, toxin A (TcdA) and toxin B (TcdB), which are the main pathogenicity factors responsible for clinical disease. Like TcdB, TcdA glucosylates rho proteins leading to actin cytoskeletal disaggregation and cytotoxicity.[4] In addition to its direct cytotoxic effects, TcdA also provokes inflammatory responses, including fluid secretion, immune cell influx, and tissue damage associated with clinical manifestations of CDI.[5–7] TcdA contains a glucosyltransferase domain, an autocatalytic cysteine protease domain, a central transmembrane domain, and a C-terminal putative receptor binding domain consisting of clostridial repetitive oligopeptides.[8] The glucosyltransferase domain is known to

*Authors share co-first authorship.

Abbreviations used in this paper: **CDI, *Clostridioides difficile* infection; CPP, cell-penetrating peptide; DMEM, Dulbecco's modified Eagle medium; IL, interleukin; PBS, phosphate-buffered saline; TcdA, *Clostridioides difficile* toxin A; SAXS, small-angle x-ray scattering; siRNA, small-interfering RNA; SUV, small unilamellar vesicle; TcdB, *Clostridioides difficile* toxin B; TLR9, Toll-like receptor 9; TNF, tumor necrosis factor; WT, wild-type.**

Most current article

© 2020 by the AGA Institute
0016-5085/$36.00
https://doi.org/10.1053/j.gastro.2020.08.038

WHAT YOU NEED TO KNOW

BACKGROUND AND CONTEXT

Clostridioides difficile toxin A (TcdA) activates the innate immune response. TcdA co-purifies with DNA. DNA binding to toll like receptor 9 (TLR9) activates the inflammatory response. This study investigated this pathway during *C difficile* infection (CDI) of mice.

NEW FINDINGS

TcdA and TcdA fragments remodel membranes, which allows them to access endosomes. TcdA fragments bound to and organized DNA for amplified activation of TLR9.

LIMITATIONS

This study was performed in cell lines, human tissues, and mice; further studies are needed in humans.

IMPACT

Rather than preventing DNA from binding TLR9, TcdA chaperones and organizes DNA into an inflammatory, spatially periodic structure.

escape from the endosome to catalyze the glycosylation of Rho-GTPases in the cytosol, leading to cytoskeletal disaggregation and cell death.[4] Studies of these translocation events for both TcdA and TcdB have concentrated on the translocation domain,[9–15] and shown that the cholesterol content of the membrane is important.[16,17] Interestingly, electrophysiology experiments have distinguished TcdA and TcdB from other pH-dependent toxins that form stable pores: both *C difficile* toxins exhibit a “flickering” conductance believed to be caused by transient pore formation.[18] TcdA also potently activates a marked innate immune response, including activation of the inflammasome, NF-κB and MAP kinases and induces a marked inflammatory response in the human colon.[5,19–21] Here we report that TcdA forms a stable complex with DNA and facilitates DNA membrane translocation. Because Toll-like receptor 9 (TLR9) recognizes intracellular CpG DNA and triggers an inflammatory response,[22] we examined the role of TLR9 in CDI pathogenesis using in vitro, in vivo models, and human colonic explants combined with machine learning and synchrotron x-ray diffraction structural studies.

BASIC AND TRANSLATIONAL AT

Materials and Methods

Machine-Learning Based Screening of Clostridioides difficile *Toxin A for Membrane-Active Sequences*

Using a previously published Support Vector Machine classifier from our laboratory,[23] we screened the full amino acid sequence of TcdA from *C difficile* for the presence of membrane-active sequences (data not included). Candidate peptides were identified by scoring individual sequences with a variable size window. Of high-scoring sequence candidates, we identified a 24–amino acid fragment in the membrane targeting N-terminal 4-helix bundle, TcdA (57–80), which we refer to as $TcdA_{57–80}$.

Small-Angle X-Ray Scattering Experiments for Peptide–Membrane Interaction

Stock solutions of 1,2-dioleoyl-*sn*-glycero-3-phosphoethanolamine, 1,2-dioleoyl-*sn*-glycero-3-phospho-L-serine (sodium salt) and cholesterol were prepared from lyophilized lipids obtained from Avanti Polar Lipids (Alabaster, AL) and dissolved in chloroform to a 20-mg/mL concentration. A lipid composition of 1,2-dioleoyl-*sn*-glycero-3-phospho-L-serine/1,2-dioleoyl-*sn*-glycero-3-phosphoethanolamine/cholesterol at a molar ratio of 20:70:10 was prepared from the stock solutions, and first evaporated under nitrogen before an overnight desiccation under vacuum. The remaining lipid film was resuspended to a concentration of 20 mg/mL in aqueous buffer solution at 2 different pH levels: 140 mM NaCl + 10 mM HEPES (pH 7.4) and 140 mM NaCl + 10 mM sodium acetate (pH 5.0). The suspensions were incubated overnight at 37°C. Subsequently, sonication was used to form small unilamellar vesicles (SUVs) suspensions. To select for vesicle size, the SUVs were extruded through a 0.2-μm pore Whatman nucleopore filter (Sigma-Aldrich, St Louis, MO). The synthesized TcdA fragment, $TcdA_{57–80}$, was purchased from LifeTein (Somerset, NJ). The lyophilized peptide was solubilized into either the pH 7.4 or pH 5 aqueous buffer, as described above for the SUV suspensions. Solubilized peptide was mixed with the matching pH buffer SUV suspensions at specified peptide to lipid charge ratio and incubated at room temperature overnight; subsequently, the samples were loaded and hermetically sealed into 1.5-mm glass capillaries (Mark-tubes; Hilgerberg GmbH, Malsfeld, Germany). Small-angle X-ray scattering (SAXS) experiments were carried out at Stanford Synchrotron Radiation Lightsource (BL 4-2) with monochromatic x-rays of energy 9 keV. Samples were incubated at 37°C and centrifuged before measurement. The scattering signature of the samples were collected using a Pilatus3 X 1M detector (pixel size 172 μm). The resulting 2-dimensional SAXS power patterns were integrated using Nika 1.50[24] package for Igor Pro 6.31 and FIT2D.[25]

The integrated SAXS intensities $I(q)$ vs q were plotted using MATLAB software. The correlation peaks corresponding to each characteristic phase (lamellar, hexagonal, and cubic) were indexed according to the characteristic peak ratios permitted for each phase: lamellar index ratios, 1:2:3; hexagonal index ratios, $\sqrt{1}:\sqrt{3}:\sqrt{4}:\sqrt{7}:\sqrt{9}:\sqrt{11}:\sqrt{12}$; and cubic (*Pn3m*) index ratios, $\sqrt{2}:\sqrt{3}:\sqrt{4}$. The corresponding measured Bragg peaks positions, $q_{measured}$, were used to fit a linear regression through the scatter plot of $q_{measured}$ against their respective Miller indices. For hexagonal phases, this corresponds to fitting equation $q = (4\pi/(a\sqrt{3}))\sqrt{(h^2 + hk + k^2)}$ for the q_{measured} vs $\sqrt{(h^2 + hk + k^2)}$ plot, and solving for the slope to obtain the lattice parameter a. Similarly, the cubic *Pn3m* phase is fitted to equation $q = (2\pi/a)\sqrt{(h^2 + hk + l^2)}$ for the q_{measured} vs $\sqrt{(h^2 + k^2 + l^2)}$ plot, and solving for a. Finally, the negative Gaussian curvature present in the cubic phase was calculated using the equation $<K> = 2\pi\chi/A_0\alpha^2$, where χ is the Euler characteristic and A_0 is the surface area per cubic unit cell for each phase. Parameter values are $\chi = -2$ and $A_0 = 1.919$ for *Pn3m* cubic phases.

Cell Lines and Clostridioides difficile *Toxin A Labeling*

Human intestinal cell lines HT-29 and THP-1 human monocyte cells were purchased from ATCC (Manassas, VA). Wild-type and TLR9 knockout mouse macrophage cell lines were collected as we described previously[26] and HEK293 wild-type (WT) cell lines were acquired from BEI Resources (Manassas, VA). TcdA was purified from *C difficile* strain VPI 10463 (ATCC). Culture supernatant was fractionated by anion-exchange chromatography, and TcdA was isolated by precipitation in acetate buffer as described previously.[27] TcdA was labeled using an Alexa Fluor 555 Protein Labeling kit (Molecular Probes, Inc, Eugene, OR) according to the manufacturer's protocol. Briefly, TcdA in TE buffer was eluted through a PD-10 column equilibrated prior with phosphate-buffered saline (PBS) to remove Tris-HCL buffer, and 0.5 mL TcdA (1.7 mg) in PBS was mixed with 50 μL 1M sodium bicarbonate and 1 vial of reactive dye. The mixture was stirred at room temperature for 1 hour and unlabeled free dye was removed by resin column chromatography.

DNA Uptake Assay

HT-29 cells were trypsinized and cell density was adjusted to 5×10^5 cell/mL in the complete Dulbecco's modified Eagle medium (DMEM), seeded on a chamber slide, and incubated for 24 hours. Bacterial source Label IT FITC Plasmid (Mirus Bio LLC, Madison, WI) was incubated with TcdA or TE buffer at room temperature for 30 minutes and diluted in DMEM to 1 μg/mL plasmid with or without 100 nM TcdA-Alexa 555. Cells were treated with DMEM (control), plasmid only and plasmid-TcdA mixture at 37°C for 2 hours in a 5% CO_2 incubator. At the end of incubation, supernatant was aspirated and cells were washed with PBS twice and fixed with CytoFix (BD, Franklin Lakes, NJ) at 4°C for 15 minutes. After washing with PBS twice, the slide was mounted with ProLong Gold antifade reagent with 4′,6-diamidino-2-phenylindole (Molecular Probes, Inc). The DNA uptake was observed by confocal microscopy.

Inhibition of TLR9 by its Antagonist ODN TTAGGG

HT-29 cells were trypsinized, cell density was adjusted to 2×10^6 cell/mL in complete DMEM medium, cells seeded in a 96-well plate, and incubated for 24 hours. The medium was replaced by serum-free DMEM for 12 hours, after which the medium was changed again to fresh serum-free medium containing TcdA, ODN TTAGGG, or their mixtures for 14 hours. THP-1 cells were maintained in complete RPMI-1640 medium. Before experiments, cells were harvested, resuspended in serum-free RPMI-1640 medium at 7×10^5 cells/mL and incubated for 12 hours. Cells were then dispensed in a 96-well plate at 1×10^6 cells/well and treated with TcdA, ODN TTAGGG, or their mixtures diluted in serum-free RPMI-1640 medium for 4 hours. At the end of treatment, the supernatants were collected for measuring interleukin (IL) 8 concentrations or for cell viability assay.

Transient Inhibition of Toll-Like Receptor 9 With Small-Interfering RNA

HT-29 cells were reverse-transfected with 50 nM TLR9 small-interfering RNA (siRNA) according to the manufacturer's instructions. Briefly, Silencer Select TLR9 siRNA (sense: 5′-CUGGAAGAGCUAAACCUGATT-3′, antisense: 5′-UCAGGUUUAG-CUCUUCCAGGG-3′) or Silencer Select Negative Control siRNA (Ambion Inc, Austin, TX) were mixed with Lipofectamine RNAiMAX (ThermoFisher Scientific, Waltham, MA), and incubated for 30 minutes at room temperature. Then, in a 24-well plate, each 100 μL of the complexes was mixed with 600 μL HT-29 cell suspension (4×10^5cell/mL) to reach 50 nM siRNA concentration and cells were incubated for 48 hours before treatment.

Transfection of Toll-Like Receptor 9 Plasmids With an Interleukin 8 Promoter and Luciferase Assay

TLR9 WT, 2 mutants (Del_Ins2 and K51M), and pcDNA3.1 vector control plasmids were acquired from Dr Alexander Dalpke, University of Heidelberg. To determine the activation of NF-κB/IL-8 in response to TLR9 recognition by TcdA, HEK293 WT cells that do not express TLR9 were transfected with WT TLR9 plasmids, each of the 2 TLR9 mutants, or pcDNA3.1 as a control using Lipofectamine LTX (Life Technologies, Inc, Carlsbad, CA) according to the manufacturer's instructions. Briefly, 0.75×10^5 cells in 0.5 mL complete growth medium were seeded in a 24-well plate for 24 hours. Cells in each well were then transfected with 0.5 μg TLR9 plasmid or vector, along with 0.1 μg NF-κB/IL-8 for 48 hours. Then the transfected cells were serum-starved for 24 hours followed by exposure to TcdA (10 nM) for 4 hours. A dual-luciferase reporter assay kit (Promega, Madison, WI) was used to measure firefly luciferase activities in cell lysate. The relative luciferase activity was then calculated by normalizing the NF-κB/IL-8 promoter-driven firefly luciferase activity of cells transfected with TLR9 plasmids against that of control cells transfected with vector.

Small-Angle X-Ray Scattering Experiments for DNA-Peptide Complex

A stock solution of double-stranded DNA was prepared from *Escherichia coli* genomic DNA (ThermoScientific, Waltham, MA) was precipitated and resuspended in aqueous solution of 140 mM NaCL + 10 mM HEPES (pH 7.4) buffer to a concentration of 5 mg/mL; the lyophilized $TcdA_{57-80}$ peptide (Life-Tein) was solubilized using the pH 7.4 buffer to stock concentration of 10 mg/mL. The DNA-peptide complex was formed by mixing the peptide with the DNA to the desired peptide to DNA charge ratio. The complex was thoroughly mixed overnight and incubated at room temperature. After equilibration, the complex was transferred to a 1.5-mm quartz capillary (Mark-tubes) and hermetically sealed. SAXS measurements were performed at the Stanford Synchrotron Radiation Lightsource (beamline 4-2) using monochromatic x-rays with an energy of 9 keV. The scattered x-rays were measured using a Pilatus3 X 1M detector (pixel size 172 μm). The

collected 2-dimensional powder diffraction patterns were radially integrated using the Nika 1.50[24] package for Igor Pro 6.31 and FIT2D.[25] The output curves were visualized using MATLAB software. The structure of the $TcdA_{57-80}$–DNA complex was solved by calculating ratios between the measured q position, $q_{measured}$, of the peaks; the observed peaks closely corresponded to $\sqrt{1}:\sqrt{3}$, which are index ratios permitted by a hexagonal columnar lattice. The lattice parameter of inter-DNA spacing, d, was calculated using a linear regression to fit equation $q = (4\pi/(d\sqrt{3}))\ \sqrt{(h^2 + hk + k^2)}$. The fit is calculated from points corresponding to q_{measured} and $\sqrt{(h^2 + hk + k^2)}$ for the Miller indices (h, k).

Experimental Animals

Female CD1, C57BL/6 WT, and TLR9 mutant (C57BL/6J-Tlr9M7Btlr/Mmjax) mice were purchased from Jackson Laboratory (Bar Harbor, ME) at 8 or 12 weeks old. Mice were housed and handled according to the protocol approved by the Beth Israel Deaconess Medical Center's institutional animal care and use committee.

Mouse Ileal Loop Assay of Clostridioides difficile *Toxin A Enterotoxicity*

Female CD1 mice of 12 weeks old were divided into 4 groups of 6. Each mouse was anesthetized and a closed, distal ileal loop (about 3 cm in length) formed at laparotomy. The loop lumen was injected with 10 μg of TcdA in 100 μL with or without ODN TTAGGG (50 μM) diluted in DMEM. ODN TTAGGG (50 μM) or medium were used as controls. The closed ileal loops were harvested and their weight to length ratios determined as a measure of enterotoxicity as described previously.[20] The ileal loop model was also used to compare TcdA-induced enterotoxicity in C57BL/6 WT and in TLR9 mutant female mice. WT and mutant mice were cohoused for 1 week before ileum loop experiment. The loop lumen of the WT and of the TLR9 mutant mice was injected with 10 μg of TcdA in DMEM or with medium alone and loop weight to length ratios were determined after 4 hours (n = 9 per group).

Antibiotic-Associated Clostridioides difficile *Infection Mouse Model*

The mouse antibiotic-associated CDI model was employed as reported previously.[28] Briefly, 8-week-old, female, C57BL6 mice (Jackson Laboratory) were divided into 2 groups (n = 10 per group). Mice were challenged with 1×10^5 cfu *C difficile* (strain VPI 10463) by gavage. E6446 (60 mg/kg/d) was given by gavage for 5 days starting on the same day of clindamycin administration. The control group received autoclaved water.

Ex Vivo Human Colonic Mucosal Biopsy Culture and Cytokine Measurement

Human colonic mucosa was obtained by forceps biopsy from the distal colon of healthy volunteers undergoing screening colonoscopy according to a protocol approved by the Committee on Clinical Investigation of Beth Israel Deaconess Medical Center. Biopsies were washed with ice-cold plain medium and immediately transferred to a 24-well plate. Each biopsy well contained 0.5 mL RPMI-1640 with 100 U/mL penicillin and 100 μg/mL streptomycin that contained TcdA (1 or 10 μg/mL) with or without ODN TTAGGG (10 μM). The cultures were maintained in 95% O_2 and 5% CO_2 at 37°C for 24 hours. The supernatants were then harvested for cytokine measurements using MILLIPLEX MAP Human Cytokine/Chemokine Magnetic Bead Panel assays (MilliporeSigma, Burlington, MA) that measured 14 inflammatory cytokines simultaneously (ie, interferon [IFN]-alfa2, IFN-gamma, IL-10, IL-1RA, IL-1α, IL-1β, IL-2, IL-4, IL-6, IL-8, MCP-1, RANTES, tumor necrosis factor [TNF]–α and TNF-β).

Statistical Analysis

Data are presented as mean ± SEM (unless otherwise specified) of at least 2 individual experiments. Comparisons between 2 groups were analyzed using Student *t* test. Analysis of variance with post–Newman-Keuls multiple comparison test was used for comparison of multiple groups. Survival results were analyzed using a Gehan–Breslow–Wilcoxon test. A *P* value $<.05$ was considered to be statistically significant.

Results

Clostridioides difficile *Toxin A Binds DNA and Facilitates Cellular Entry*

Upon purification of TcdA from *C difficile*, we found that DNA is co-purified with the toxin at a 0.06% ± 0.02% DNA concentration (0.6 μg DNA per mg toxin protein). The presence of DNA was observed in both native and recombinant toxins from multiple academic and commercial sources. DNA was extracted, followed by polymerase chain reaction and sequencing, and identified to be *C difficile* genomic DNA and other contaminating DNAs. To examine the DNA binding ability of TcdA directly, DNA fragments with various sizes (1 kb DNA ladder) were incubated with TcdA, which markedly lowered DNA marker mobility in gel electrophoresis (Figure 1*A*). Moreover, digestion by DNase I only leads to a 12% decrease in DNA, suggesting a stable protein–DNA complex that resists DNase digestion. This indicates a capacity for stable complex formation between DNA and TcdA (or fragments thereof) that may protect DNA from enzymatic degradation.

TcdA is hypothesized to undergo receptor-mediated endocytosis,[8] although its specific surface receptors and cell entry mechanism remain elusive.[29] Therefore, to systematically discover potential parallel pathways of translocation, we analyzed the entire TcdA protein sequence using a recently developed machine learning classifier.[23,30,31] Surprisingly, although recent empirical work has identified cell-penetrating peptide (CPP)-like domains along the translocation domain,[11,12] the classifier identified multiple new regions of TcdA that are expected to have direct membrane remodeling activity reminiscent of CPPs, including regions far from the translocation domain. These results suggested that TcdA is unusual in that it possesses multiple CPP domains that facilitate membrane translocation (such as that involved in cell entry and endosomal egress). We examined experimentally a 24aa peptide fragment ($TcdA_{57-80}$) in the N-terminal 4-helix bundle of the glycosyl-transferase domain (Figure 1*B*), as it has been described previously to be membrane targeting.[32,33] To

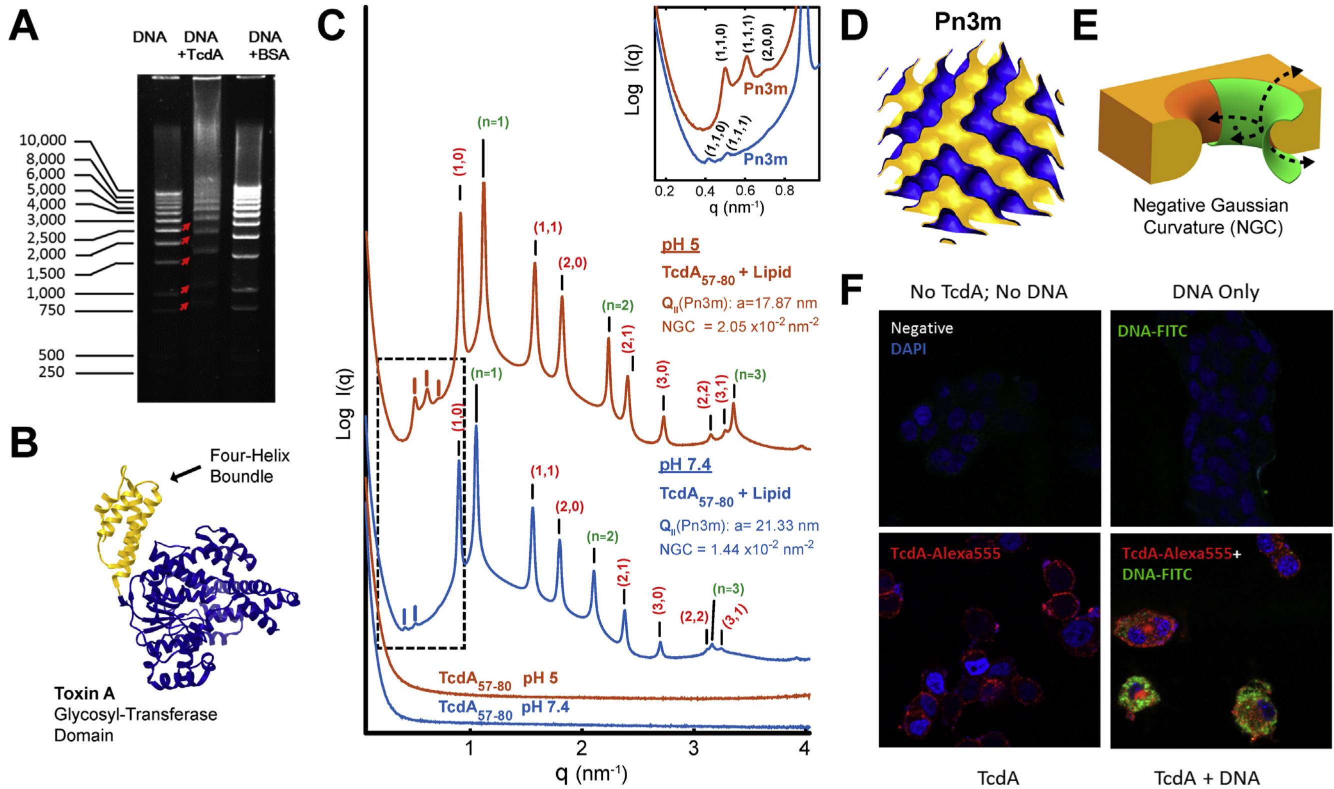

Figure 1. *C difficile* TcdA binds DNA and facilitates DNA's cellular entry. (*A*) TcdA binds to DNA. Gel electrophoresis showing that the incubation of TcdA (10 μg) with a 1-kb DNA ladder (2 μg) retarded DNA mobility. Incubation of DNA with bovine serum albumin (BSA) (10 μg) acted as a negative control. (*B*) Four-helix bundle in the glucosyltransferase domain. Solved 3-dimensional (3D) crystal structure of the N-terminal glucosyltransferase domain from TcdA (PDB ID: 4DMV), highlighting the position of the membrane targeting N-terminal 4-helix bundle motif (*yellow*). (*C*) TcdA 4-helix bundle segment, $TcdA_{57–80}$, generates negative Gaussian curvature (NGC) necessary for membrane permeabilization. SAXS spectra from 20/70/10 phosphatidylserine (PS)/phosphatidylethanolamine (PE)/cholesterol (Chl) model membranes incubated with $TcdA_{57–80}$, at a 1:4 peptide to lipid charge ratio. At both pH 7.4 and pH 5.0, $TcdA_{57–80}$ induces NGC in the form of a *Pn3m* Q_{II} cubic phase (*insert plot*). The additional observed reflections for the positive curvature hexagonal (*red indices*) and lamellar (*green indices*) phases have been assigned on the curves, with periodicity of 8.0 and 5.7 nm at pH 5, and 8.1 and 6.0 nm at pH 7.4, respectively. No Bragg reflections were observed for the peptide solutions alone (*bottom*). Only hexagonal phases were present for the membrane SUVs suspensions at both pHs (Supplementary Figure 1). To facilitate visualization, spectra have been manually offset vertically by a multiplicative factor. (*D*) Reconstruction of a Pn3m surface. 3D reconstruction depicting a Pn3m Q_{II} cubic phase, with continuous surfaces forming NGC at every point. (*E*) Illustration of NGC geometry. 3D rendering of the saddle-splay inherent to negative Gaussian curvature geometry (*green*) as superimposed on a mechanism of membrane remodeling. (*F*) TcdA facilitates cellular uptake of DNA. HT29 colonic epithelial cells were treated with medium (negative) or DNA-fluorescein isothiocyanate (FITC) (1 μg/mL, *green*) alone or along with Alexa 555 labeled TcdA (100 nM, *red*) for 2 hours at 37°C. Cells were fixed with Cyto-Fix at 4°C for 15 minutes and nuclei were stained with 4′,6-diamidino-2-phenylindole (*blue*). Significantly increased plasmid DNA was observed in the cytosol of TcdA-treated colonocytes (*bottom right panel*).

investigate membrane deformations induced by $TcdA_{57–80}$, we incubated the fragment with SUVs prepared from ternary phospholipid mixtures of phosphatidylserine, phosphatidylethanolamine, and cholesterol at a stoichiometry of phosphatidylserine/phosphatidylethanolamine/cholesterol = 20/70/10, and examined the resultant peptide-membrane structure using SAXS (Figure 1*C*). Interestingly, in addition to lamellar and inverted hexagonal phases, we observed the formation of a *Pn3m* bicontinuous cubic (Q_{II}) phase at both neutral pH 7.4 and at acidic pH 5, with lattice parameters of 17.87 and 21.33 nm, respectively (Figure 1*C* and *D*). This observed peptide-induced membrane remodeling is homologous to that observed for HIV TAT, the canonical CPP[34]. The measured *Pn3m* structure is rich in negative Gaussian curvature, the type of curvature that is topologically required in membrane permeation events, such as pore formation, blebbing, budding, and endocytosis (Figure 1*E*). This result indicates that this domain of TcdA, together with other previously reported CPPs of TcdA[11] are able to mediate translocation across membranes.

To test this idea further, we examined whether TcdA facilitates cellular uptake of DNA into human colonocytes. We co-treated HT29 colonic epithelial cells with TcdA (Alexa 555-labeled) and/or bacterial plasmid DNA (fluorescein isothiocyanate–labeled). Confocal imaging demonstrated

significantly increased DNA in the cytosol of TcdA-treated colonocytes, indicating that TcdA can facilitate DNA internalization (Figure 1*F*), consistent with x-ray (SAXS) and machine learning results.

Toll-Like Receptor 9 Mediates Clostridioides difficile *Toxin A–Induced Proinflammatory Response Through DNA Recognition*

As it is known that TLR9 recognizes bacterial or viral DNA and leads to pro-inflammatory reactions, including the production of proinflammatory cytokines,[22] we examined whether cellular uptake of DNA in the presence of *C difficile* TcdA results in stimulation of TLR9 pathway-associated cytokine production. We tested whether TLR9 is important in TcdA-induced cytokine production in vitro by using the TLR9 antagonist ODN TTAGGG. In THP-1 (human monocytic) cells, TcdA-induced IL-8 production was significantly suppressed by ODN TTAGGG (Figure 2*A*). ODN TTAGGG also inhibited TcdA-induced IL-8 production in HT29 (human colonic epithelial) cells (Supplementary Figure 2). Conversely, in our control experiments, ODN TTAGGG did not inhibit IL-8 productions induced by IL-1β or TNF-α, which do not act through TLR9 activation (Supplementary Figure 3). We next transiently inhibited TLR9 expression in HT29 cells by transfecting the cells with an anti-TLR9 siRNA, which also significantly reduced TcdA-induced IL-8 production compared with mock control (Figure 2*B*).

To further validate the role of TLR9 in TcdA-induced cellular responses, we compared TLR9 knockout mouse macrophages with WT control. It has been reported that TLR9 activation may lead cells to undergo apoptosis, necrosis, and pyroptosis,[35–37] but its role in TcdA-induced cell death is not known. We found that TLR9 knockout macrophages were more resistant to TcdA-induced cell death compared with WT cells (Figure 2*C*).

To further examine the role of TLR9 in TcdA-induced cytokine production, we transfected HEK-293 (TLR9 *null*) cells with human TLR9. Overexpression of WT TLR9 significantly increased NF-κB/IL-8 luciferase reporter signal in response to TcdA (Figure 2*D*). In contrast, transfection with either of 2 TLR9 mutants (Del_Ins2 or K51M) that cannot bind CpG DNAs[38] was associated with loss of the activation effect (Figure 2*D*). These findings indicate that a functioning TLR9 is essential for the signaling response induced by TcdA.

TLR9 Plays a Pivotal Role in Clostridioides difficile *Toxin A–Induced Enterotoxicity in Vivo Mouse Models*

To examine the role of TLR9 in TcdA-induced enterotoxicity in vivo, we injected the toxin into mouse ileal loops with or without the TLR9 antagonist ODN TTAGGG (Figure 3*A*). ODN TTAGGG significantly attenuated TcdA-induced fluid secretion (enterotoxicity), indicating chemical inhibition of TLR9 blocks in vivo response to TcdA in mouse intestine.

In comparison with WT mice, mice with a single nucleotide substitution that precludes TLR9 activation by CpG DNA (C57BL/6J-*Tlr9*^{M7Btlr}/Mmjax, MGI Ref ID *J:165701*) show significantly less TcdA-induced enterotoxicity (Figure 3*B*), indicating that the DNA binding domain of TLR9 contributes to, at least partially, TcdA's enterotoxicity in mouse ileum. For additional in vivo experiments, we examined the role of TLR9 activation in the infectious model of antibiotic-associated CDI.[28] Treatment with E6446, an orally stable TLR9 antagonist,[39] significantly protected mice from CDI-induced death (Kaplan–Meier analysis: $P < .05$ treated vs control) (Figure 3*C*), providing a third line of evidence for TLR9's importance in CDI in vivo.

TLR9 Inhibition Protects Human Colonic Mucosa From Clostridioides difficile *Toxin A–Induced Proinflammatory Cytokine Production*

Using ex vivo culture of freshly harvested human colonic mucosal biopsies, we examined the effects of the TLR9 antagonist ODN TTAGGG on TcdA-induced cytokine production. TcdA increased the concentrations of multiple proinflammatory cytokines in the conditioned media. The TLR9 antagonist significantly attenuated TcdA-induced proinflammatory cytokine production by the human colonic mucosal biopsies. IFN-alfa2, a known product of TLR9 activation, was increased 2.1-fold by TcdA and this increase was prevented by antagonism of TLR9 ($P < .01$). Similar inhibitory effects were also observed for other key cytokines in CDI, such as TNF-α ($P < .01$), TNF-β ($P < .05$), MCP-1 ($P < .01$), and RANTES ($P < .01$) (Figure 4*A*). These data indicate that TLR9 activation mediates innate immune responses to *C difficile* TcdA in human colon.

Immune Activation in the Extreme Case of Protease-Rich Environments That Degrade Clostridioides difficile *Toxin A Into Fragments*

An interesting question to consider for gut inflammation is what happens in protease-rich environments, such as the colonic lumen, where TcdA is partially digested into peptide fragments. We showed above that TcdA has its own protein transduction domain in addition to other CPP domains. Consistent with CPP behavior, isolated CPPs or protein transduction domains can facilitate membrane remodeling and endosomal access. Recent work has shown that it is possible for cationic amphiphilic peptides to co-assemble with double-stranded DNA into ordered nanocrystalline complexes that drastically amplify TLR9 activation.[40–42] Examples include membrane-active innate immune peptides that organize into 4-helix bundles,[42] bacterial amyloids,[41] and chemokines,[42] which all can organize and present double-stranded DNA ligands at geometric spacings that drive TLR9 receptor clustering and multivalent binding. To mimic the protease-rich environment of the gut, we do not assume the long-term persistence of any tertiary or higher-level structure (such as the N-terminal four-helix bundle). Hence, we examined the TcdA protein transduction domain fragment described above that has been

BASIC AND TRANSLATIONAL AT

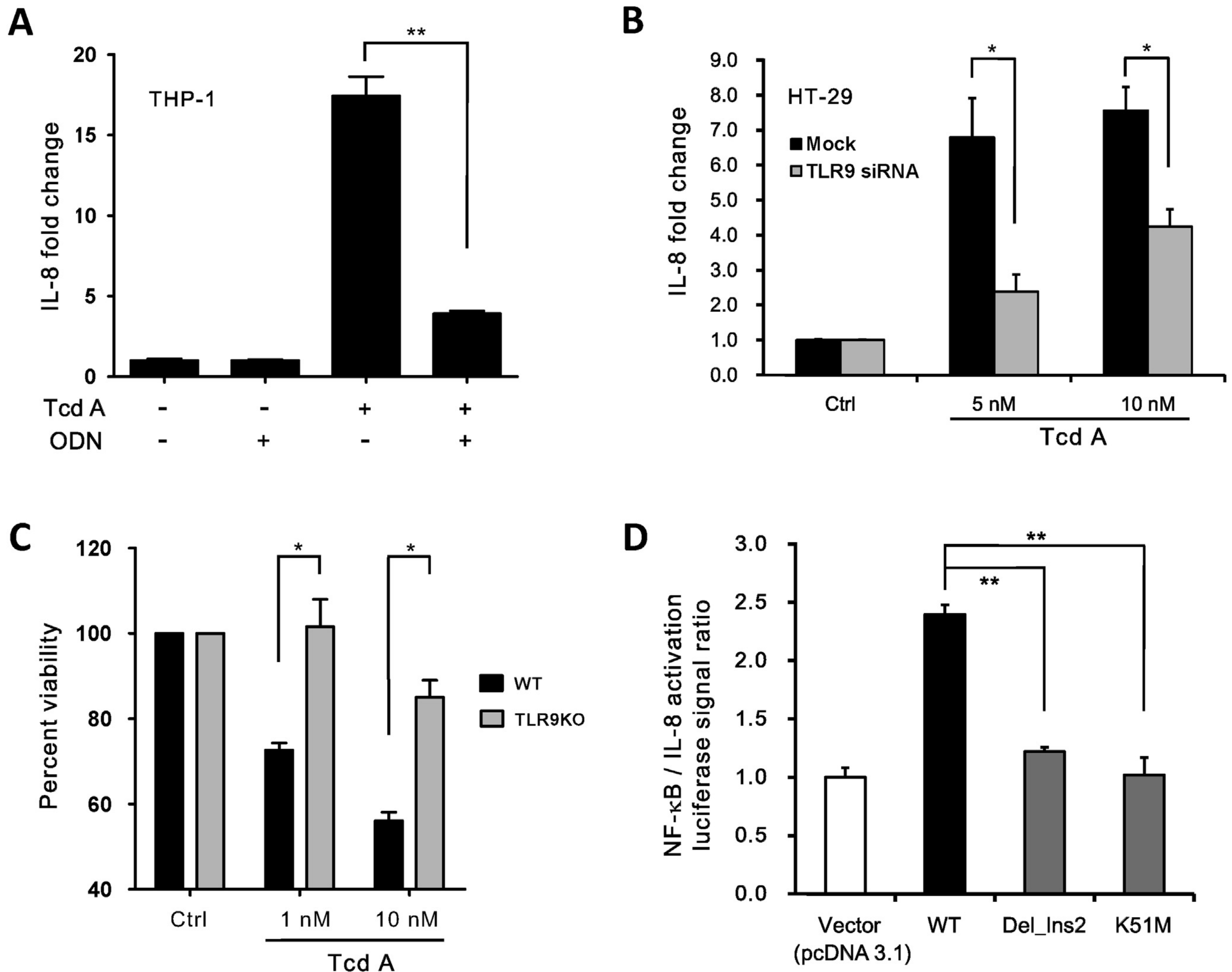

Figure 2. TLR9 mediates TcdA-induced proinflammatory response through DNA recognition (*A*). Antagonizing TLR9 attenuates TcdA-induced IL-8 production. THP-1 monocytes were treated with medium as a control (ctrl), 25 μM ODN TTAGGG (ODN), TcdA (100 nM), or TcdA together with ODN (TcdA+ODN) for 4 hours. IL-8 production was measured by enzyme-linked immunosorbent assay. $^{**}P < .01$, Student *t* test. (*B*) Silencing TLR9 translation attenuates TcdA-induced IL-8 production. HT-29 cells were transfected with TLR9 siRNA (50 nM) or negative control (mock) for 48 hours and then treated with TcdA for 14 hours. $^{*}P < 0.05$, Student *t* test. (*C*) TLR9 knock-out mouse macrophages have less cell death in response to TcdA. WT (Mf-WT) or TLR9 knockout (Mf-TLR9KO) mouse macrophages were treated with TcdA (0, 1, or 10 nM) for 24 hours. Loss of cellular viability was determined by lactate dehydrogenase release. $^{*}P < 0.05$, Student *t* test. (*D*) WT TLR9 overexpression results in increased NF-κB/IL-8 activation in HEK293 (TLR9 null) cells. This increase is abolished in cells transfected with TLR9 mutants that lack a functional DNA-recognition domain. HEK293 cells were transfected with vector (pcDNA3.1), TLR9 WT, or TLR9 mutants with either a deletion (Del_Ins2) or single nucleotide substitution mutation (K51M) that result in loss of DNA binding. After 48 hours, cells were treated with TcdA (10 nM) for 4 hours. The activation of NF-κB/IL-8 was measured by a luciferase reporter and data presented as normalized ratios. $^{**}P < .01$, Student *t* test.

shown to have the capacity for endosomal access according to our experiments (see Figure 1 and Results). We incubated genomic *Escherichia coli* double-stranded DNA with $TcdA_{57-80}$ and observed the formation of an ordered $TcdA_{57-80}$-DNA complex. SAXS measurement of the complex produced Bragg reflections at $q_{100} = 1.765$ and $q_{110} = 3.068$ nm^{-1}, indicating the formation of a columnar hexagonal DNA lattice with an inter-DNA spacing of 4.1 nm (Figure 4*B* and *C*), which is in the range of optimal values that has been shown to amplify TLR9 activation in a deterministic manner: In other words, the $TcdA_{57-80}$-DNA complex presents parallel DNA at an inter-DNA spacing that promotes binding of multiple TLR9s. Therefore, we find that even fragments of TcdA have the ability to enter endosomal compartments and optimally arrange DNA for TLR9 presentation and trigger a proinflammatory response.

Discussion

In this report, we demonstrate that *C difficile* TcdA binds to DNA, facilitates DNA entry into human colonocytes, and organizes DNA for amplified TLR9-mediated immune

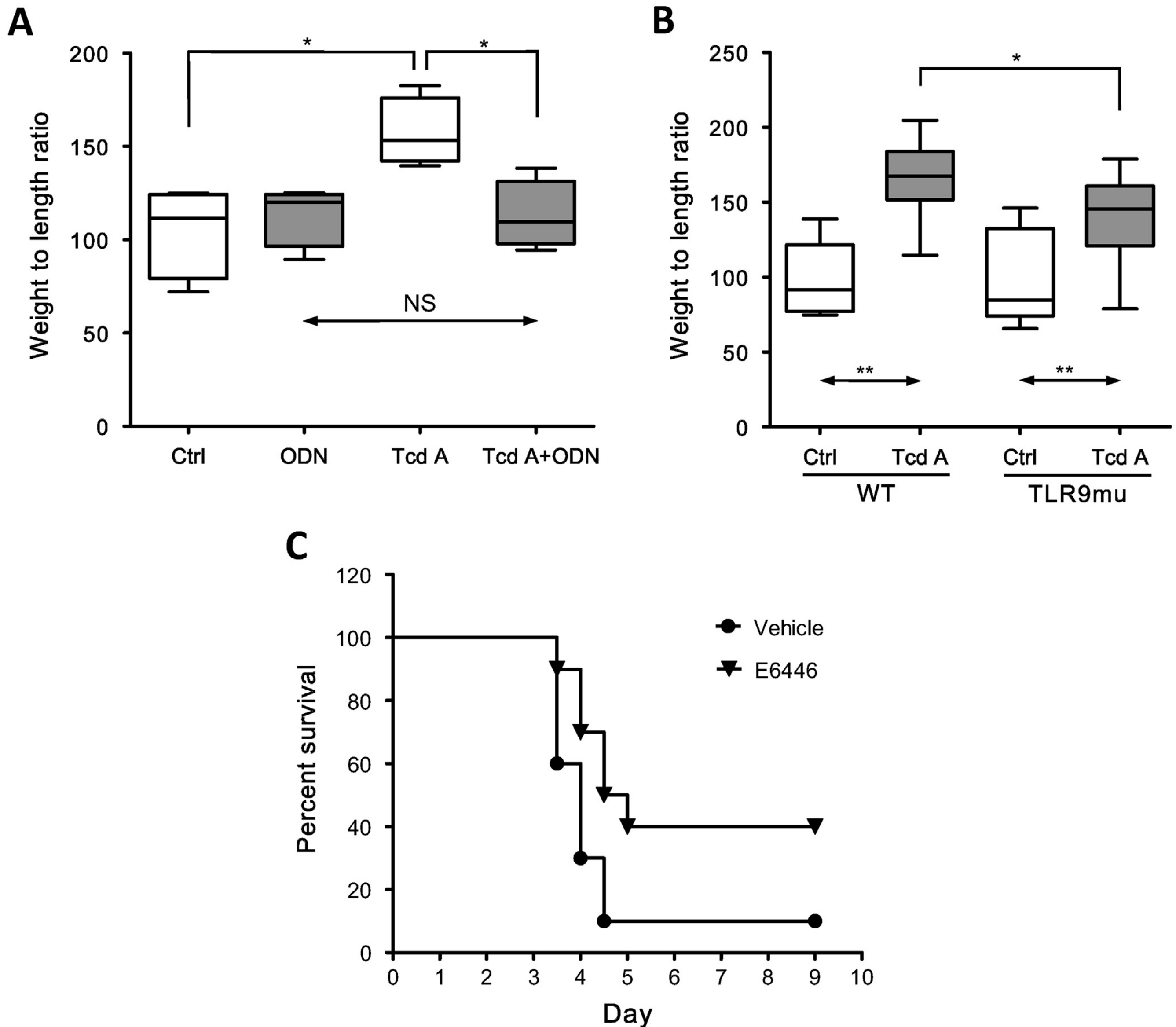

Figure 3. TLR9 plays a pivotal role in 2 in vivo CDI mouse models. (*A*) The TLR9 antagonist ODN TTAGGG inhibited TcdA-mediated enterotoxicity in mouse ileum in vivo. CD1 mice were anesthetized and closed distal ileal loops created at laparotomy. Loops were injected with 100 μL of DMEM alone (Ctrl) or DMEM containing ODN TTAGGG (50 μM, ODN), TcdA (100 μg/mL, TcdA), or TcdA (100 μg/mL) plus ODN TTAGGG (50 μM). Four hours after the injection, fluid secretion, an indicator of enterotoxicity, was estimated by determining loop weight to length ratios. Data are from a representative of 3 individual experiments and presented as median with 10th, 25th, 75th and 90th ranges (n = 6 per group, *$P < .05$; NS, not significant [$P > .05$], 1-way analysis of variance [ANOVA] with multiple comparisons). (*B*) TLR9 mutant mice show reduced TcdA-mediated enterotoxicity in mouse ileum in vivo. Wild-type C57BL6J (WT) and mutant C57BL/6J-Tlr9M7Btlr/Mmjax (TLR9mu; expressing TLR9 that is not activated by CpG DNA) were compared using mouse ileal model of CDI. As described in (*A*), the enterotoxicity of TcdA (10 μg) was assessed by loop weight to length ratios. Data were pooled from 3 independent experiments and presented as median with 10th, 25th, 75th and 90th ranges. *$P < .05$; ** $P < .01$, n = 9 each group, 1-way ANOVA with multiple comparisons. (*C*) The orally active TLR9 antagonist E6446 protected mice from antibiotic-associated CDI in vivo. The murine model of antibiotic-associated CDI was employed as described previously. C57BL6 female mice received E6446 (60 mg/kg/day orally) starting 1 day before *C difficile* challenge and for an additional 4 days or until death/sacrifice. Survival was recorded every 8 hours after challenge. Compared with vehicle, E6446 treatment significantly attenuated CDI in mice. *$P < .05$ vs vehicle. n = 10 each group. Kaplan–Meier analysis.

activation. We find multiple cell penetrating peptide motifs in TcdA that can enhance endosomal access for the toxin. TLR9 signaling was required in TcdA-induced inflammatory responses in vitro and in vivo, and in human colonic mucosa. Finally, in the extreme case of TcdA digestion into peptide fragments in the protease-rich colonic luminal environment, we find that the $TcdA_{57-80}$ protein transduction fragment capable of CPP-like membrane translocation activity can also organize bacterial DNA into a nanocrystalline complex that presents DNA ligands in

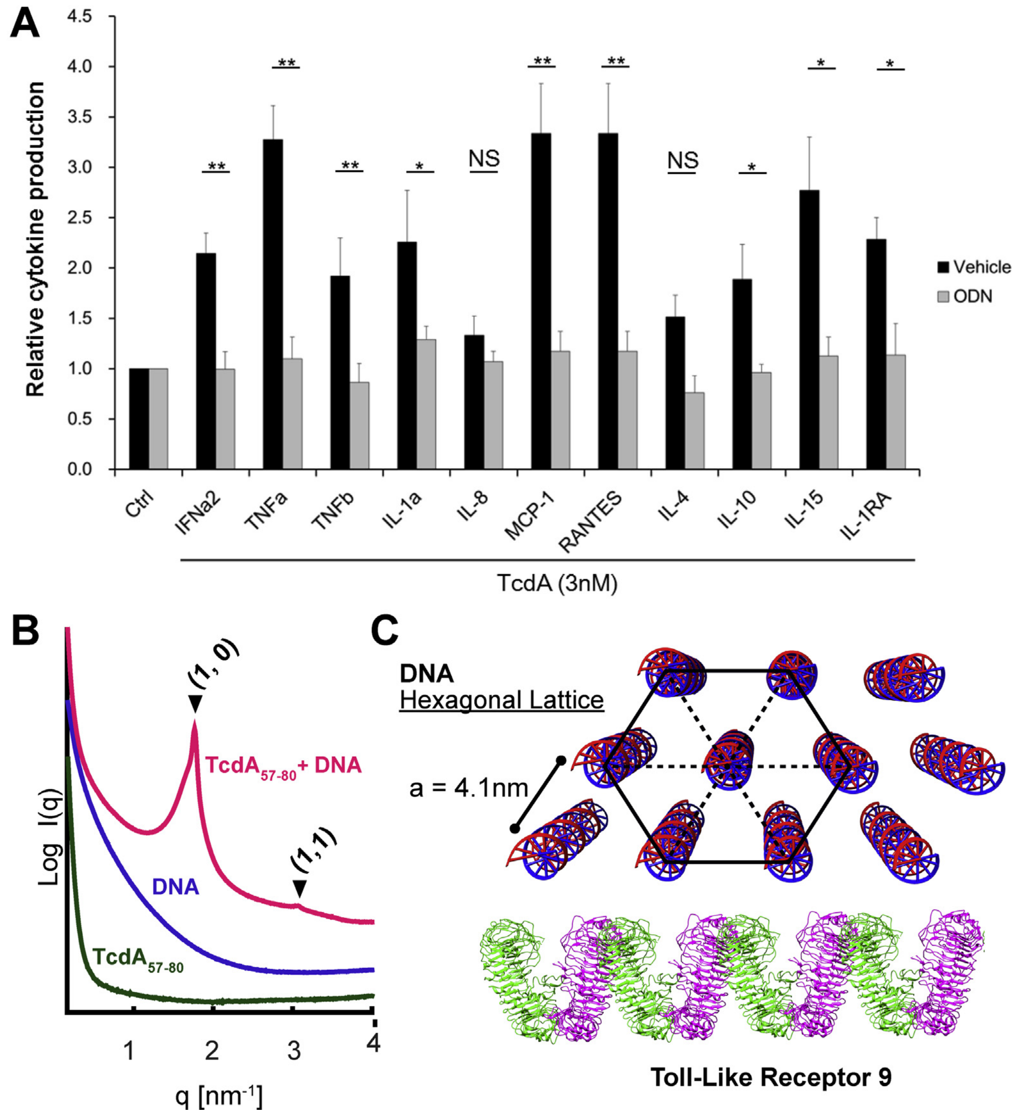

Figure 4. TLR9 inhibition protects human colonic mucosa from TcdA-induced proinflammatory cytokine induction while $TcdA_{57\text{-}80}$ fragment organized DNA into optimal lattice spacing for TLR9 activation. (*A*) Human colonic biopsies were treated with TcdA (3 nM) for 24 hours with or without ODN TTAGGG (10 nM). The cytokines/chemokines released into the conditioned media were measured by immunoassay. Data were represented as mean ± SEM. **P* < .05; ***P* < .01; NS, not significant; Student *t* test. (*B*) $TcdA_{57\text{–}80}$ fragment organizes DNA into a nanocrystalline hexagonal columnar lattice. SAXS curve of $TcdA_{57\text{–}80}$ complexed with DNA (*red*); the formed structure generated Bragg peaks corresponding to a hexagonal lattice. These reflections are not observed from the $TcdA_{57\text{–}80}$ peptide alone (*green*), or DNA in solution by itself (*violet*). All samples were tested at pH 7.4. To facilitate visualization, spectra have been manually offset vertically by a multiplicative factor. (*C*) Diagram of a DNA hexagonal lattice presented to an array of TLR9 receptors. Illustration of the proposed DNA 3-dimensional hexagonal columnar structure organized by $TcdA_{57\text{–}80}$ for TLR9 presentation.

a multivalent manner and thereby amplifies TLR9 activation.

We have identified putative DNA binding motifs dispersed across TcdA. Moreover, the binding to DNA appears to be electrostatic in origin and therefore quite general because *C difficile* genomic DNA, bacterial plasmid DNA, and bacteriophage DNA (DNA ladders) can all bind to cationic motifs in TcdA, which is already known to bind negatively charged polymers.[43] Toxins and extracellular DNA along with polysaccharides are observed as major components in the biofilm matrix of *C difficile*.[44]

The two TcdA activities that we highlight here, the ability to remodel membranes for permeation and the ability to chaperone and organize DNA for amplified TLR9 activation, are both activities identified for antimicrobial peptides.[40,45–47] These observations suggest that TcdA is capable of mimicking components of the innate immune system to amplify inflammation.

It is indeed interesting to explore why *C difficile* induces inflammation in the gut via the mechanisms described here. Although the answers for *C difficile* are not known, recent studies suggest ways in which pathogens may capitalize on

gut inflammation. In the case of *Salmonella typhimurium*, innate immune responses lead to production of reactive oxygen and nitrogen species. These in turn convert endogenous sulfur compounds to new respiratory electron acceptors that give *S typhimurium* a growth advantage over fermenting microbial species.[48] *C difficile* is anaerobic and uses different mechanisms. Recent work indicates that antibiotic-mediated disruption of native microbiota allows *C difficile* to take advantage of microbiota-liberated mucosal carbohydrates.[49] Cognate effects from inflammation may be possible. Reduction in microbial diversity will likely also impact *C difficile*'s fitness in the local ecosystem. In a larger compass, there are other cognate examples where DNA forms a cell penetrating complex that mediates pro-inflammatory outcomes. Hemozoin, an inorganic crystal produced by the protozoan parasite *Plasmodium,* is coated with malaria DNA that it presents to activate TLR9-mediated immune responses.[26] Another example is granulin, a mitogen and neurotrophic mammalian protein that has been reported to deliver CpG-DNA to the endosome and potentiate TLR9 responses.[50] *C difficile* TcdA, to our knowledge, is the first known major bacterial toxin that leads to DNA delivery into host cells to stimulate immune responses through TLR9. Given its widespread and promiscuous DNA binding motifs, it is conceivable that TcdA can also bind to colonic luminal DNA from the intestinal microbiota. Once the colonic epithelial barrier is disrupted by toxin, microbiota-derived DNA can be exposed to subepithelial cells (eg, monocytes and macrophages) resulting in a robust inflammatory reaction driven by TLR9 signaling.

The observation that even fragments of TcdA ($TcdA_{57-80}$) can function independently, showing synergistic CPP and pro-inflammatory activities, is interesting and highly suggestive of TcdA retaining these effects despite digestion by colonic luminal bacterial peptidases. Clearly, TcdA–DNA binding may not interfere with TLR9 activation; it can even amplify, as shown by recent examples.[40,42] Results here suggest that in addition to TcdA-DNA induced TLR9 activation, even TcdA fragments in the colonic lumen can bind and organize bacterial DNA into ordered complexes to activate DNA-dependent, TLR9-dependent, innate inflammatory responses. This TLR9-dependent pathway is apparently robust in the protease-rich environment of the gut, and exists in addition to the toxin's known rho glucosylation and auto-protease enzymatic activities and inflammasome activation.[19,21,51] It is tempting to hypothesize that there are likely other TcdA fragments with similar composite activity; by comparison, there are many antimicrobial peptides with cognate ability to organize DNA and activate TLR9.[42] In recent studies, the regulation of proteases (from both the host and microflora) has been linked to pathogenesis of gastrointestinal autoimmune and inflammatory diseases.[52,53] Moreover, due to the rich diversity of proteases in the gut, we hypothesize that there exists a range of pro-inflammatory mechanisms cognate to the one that we have identified, which involve entry of some toxin derivative or fragment with DNA.

The findings here introduce TcdA-DNA binding and TLR9 activation as novel pathogenic events and potential treatment targets, in *C difficile* infection. Our data unambiguously demonstrate the impact of TLR9 signaling on TcdA-mediated damage and inflammation in vitro, in the mouse gut in vivo and in human colon biopsies. It is therefore interesting to consider the source of DNA used for pathologic TLR9 activation. Given the abundance of bacterial DNAs in gut lumen and the promiscuous nature of electrostatic binding, it is likely that the gut commensal bacterial DNA, facilitated by CPP activity of toxin fragments, may enter gut epithelial cells, macrophages, and monocytes, activate TLR9 signaling and therefore exacerbate further the inflammatory responses initiated by toxin's enzymatically mediated, intrinsic, enterotoxicity and cytotoxicity, leading to damage to the gut barrier. Recent work, however, indicates that even mammalian DNA organized in nanocrystalline complexes similar to those observed here can also activate TLR9 and this phenomenon has been implicated in autoimmune diseases.[40–42] This suggests that endogenous DNA from damaged epithelial cells can also contribute to TLR9 activation.

Supplementary Material

Note: To access the supplementary material accompanying this article, visit the online version of *Gastroenterology* at www.gastrojournal.org, and at https://doi.org/10.1053/j.gastro.2020.08.038.

References

1. Kelly CP, LaMont JT. *Clostridium difficile*—more difficult than ever. N Engl J Med 2008;359:1932–1940.
2. Chen X, Lamont JT. Overview of *Clostridium difficile* infection: implications for China. Gastroenterol Rep (Oxf) 2013;1:153–158.
3. Burke KE, Lamont JT. *Clostridium difficile* infection: a worldwide disease. Gut Liver 2014;8:1–6.
4. Just I, Selzer J, Wilm M, et al. Glucosylation of Rho proteins by *Clostridium difficile* toxin B. Nature 1995;375:500–503.
5. Kelly CP, Kyne L. The host immune response to *Clostridium difficile*. J Med Microbiol 2011;60:1070–1079.
6. Voth DE, Ballard JD. *Clostridium difficile* toxins: mechanism of action and role in disease. Clin Microbiol Rev 2005;18:247–263.
7. Vedantam G, Clark A, Chu M, et al. *Clostridium difficile* infection: toxins and non-toxin virulence factors, and their contributions to disease establishment and host response. Gut Microbes 2012;3:121–134.
8. Jank T, Aktories K. Structure and mode of action of clostridial glucosylating toxins: the ABCD model. Trends Microbiol 2008;16:222–229.
9. Chen S, Wang H, Gu H, et al. Identification of an essential region for translocation of *Clostridium difficile* toxin B. Toxins (Basel) 2016;8(8):241.
10. Zhang Z, Park M, Tam J, et al. Translocation domain mutations affecting cellular toxicity identify the *Clostridium difficile* toxin B pore. Proc Natl Acad Sci U S A 2014;111:3721–3726.

11. Larabee JL, Hauck GD, Ballard JD. Cell-penetrating peptides derived from *Clostridium difficile* TcdB2 and a related large clostridial toxin. J Biol Chem 2018; 293:1810–1819.
12. Larabee JL, Bland SJ, Hunt JJ, et al. Intrinsic toxin-derived peptides destabilize and inactivate *Clostridium difficile* TcdB. mBio 2017;8(3):e00503–e00517.
13. Hamza T, Zhang Z, Melnyk RA, et al. Defective mutations within the translocation domain of *Clostridium difficile* toxin B impair disease pathogenesis. Pathog Dis 2016; 74:ftv098.
14. Orrell KE, Mansfield MJ, Doxey AC, et al. The *C. difficile* toxin B membrane translocation machinery is an evolutionarily conserved protein delivery apparatus. Nat Commun 2020;11:432.
15. Manse JS, Baldwin MR. Binding and entry of *Clostridium difficile* toxin B is mediated by multiple domains. FEBS Lett 2015;589:3945–3951.
16. Giesemann T, Jank T, Gerhard R, et al. Cholesterol-dependent pore formation of *Clostridium difficile* toxin A. J Biol Chem 2006;281:10808–10815.
17. Papatheodorou P, Song S, López-Ureña D, et al. Cytotoxicity of *Clostridium difficile* toxins A and B requires an active and functional SREBP-2 pathway. FASEB J 2019; 33:4883–4892.
18. Barth H, Pfeifer G, Hofmann F, et al. Low pH-induced formation of ion channels by *Clostridium difficile* toxin B in target cells. J Biol Chem 2001;276:10670–10676.
19. Ng J, Hirota SA, Gross O, et al. *Clostridium difficile* toxin-induced inflammation and intestinal injury are mediated by the inflammasome. Gastroenterology 2010;139:542–552; 552.e1–3.
20. Warny M, Keates AC, Keates S, et al. p38 MAP kinase activation by *Clostridium difficile* toxin A mediates monocyte necrosis, IL-8 production, and enteritis. J Clin Invest 2000;105:1147–1156.
21. Xu H, Yang J, Gao W, et al. Innate immune sensing of bacterial modifications of Rho GTPases by the Pyrin inflammasome. Nature 2014;513(7517):237–241.
22. Kumagai Y, Takeuchi O, Akira S. TLR9 as a key receptor for the recognition of DNA. Adv Drug Deliv Rev 2008; 60:795–804.
23. Lee EY, Fulan BM, Wong GCL, et al. Mapping membrane activity in undiscovered peptide sequence space using machine learning. Proc Natl Acad Sci U S A 2016; 113:13588–13593.
24. Ilavsky J. Nika: software for two-dimensional data reduction. J Appl Crystallography 2012;45:324–328.
25. Hammersley AP. FIT2D: An Introduction and Overview. Internal Report No. ESRF97HA02T European Synchrotron Radiation Facility. Grenoble: France, 1997.
26. Parroche P, Lauw FN, Goutagny N, et al. Malaria hemozoin is immunologically inert but radically enhances innate responses by presenting malaria DNA to Toll-like receptor 9. Proc Natl Acad Sci U S A 2007;104:1919–1924.
27. Sullivan NM, Pellett S, Wilkins TD. Purification and characterization of toxins A and B of *Clostridium difficile*. Infect Immun 1982;35:1032–1040.
28. Chen X, Katchar K, Goldsmith JD, et al. A mouse model of *Clostridium difficile*-associated disease. Gastroenterology 2008;135:1984–1992.
29. Tao L, Tian S, Zhang J, et al. Sulfated glycosaminoglycans and low-density lipoprotein receptor contribute to *Clostridium difficile* toxin A entry into cells. Nat Microbiol 2019;4:1760–1769.
30. Silvestre-Roig C, Braster Q, Wichapong K, et al. Externalized histone H4 orchestrates chronic inflammation by inducing lytic cell death. Nature 2019;569:236–240.
31. Lee MW, Lee EY, Lai GH, et al. Molecular Dnm1 synergistically induces membrane curvature to facilitate mitochondrial fission. ACS Central Sci 2017;3:1156–1167.
32. Geissler B. Bacterial toxin effector-membrane targeting: outside in, then back again. Front Cell Infect Microbiol 2012;2:75.
33. Geissler B, Tungekar R, Satchell KJF. Identification of a conserved membrane localization domain within numerous large bacterial protein toxins. Proc Natl Acad Sci U S A 2010;107:5581–5586.
34. Mishra A, Lai GH, Schmidt NW, et al. Translocation of HIV TAT peptide and analogues induced by multiplexed membrane and cytoskeletal interactions. Proc Natl Acad Sci U S A 2011;108:16883–16888.
35. Krysko DV, Kaczmarek A, Krysko O, et al. TLR-2 and TLR-9 are sensors of apoptosis in a mouse model of doxorubicin-induced acute inflammation. Cell Death Differ 2011;18:1316–1325.
36. Jaiswal MK, Agrawal V, Mallers T, et al. Regulation of apoptosis and innate immune stimuli in inflammation-induced preterm labor. J Immunol 2013;191:5702–5713.
37. Bortoluci KR, Medzhitov R. Control of infection by pyroptosis and autophagy: role of TLR and NLR. Cell Mol Life Sci 2010;67:1643–1651.
38. Peter ME, Kubarenko AV, Weber AN, et al. Identification of an N-terminal recognition site in TLR9 that contributes to CpG-DNA-mediated receptor activation. J Immunol 2009;182:7690–7697.
39. Franklin BS, Ishizaka ST, Lamphier M, et al. Therapeutical targeting of nucleic acid-sensing Toll-like receptors prevents experimental cerebral malaria. Proc Natl Acad Sci U S A 2011;108:3689–3694.
40. Schmidt NW, Jin F, Lande R, et al. Liquid-crystalline ordering of antimicrobial peptide–DNA complexes controls TLR9 activation. Nat Mater 2015;14:696.
41. Tursi SA, Lee EY, Medeiros NJ, et al. Bacterial amyloid curli acts as a carrier for DNA to elicit an autoimmune response via TLR2 and TLR9. PLoS Pathog 2017;13: e1006315.
42. Lande R, Lee EY, Palazzo R, et al. CXCL4 assembles DNA into liquid crystalline complexes to amplify TLR9-mediated interferon-α production in systemic sclerosis. Nat Commun 2019;10:1731.
43. Braunlin W, Xu Q, Hook P, et al. Toxin binding of tolevamer, a polyanionic drug that protects against antibiotic-associated diarrhea. Biophys J 2004;87:534–539.

44. Semenyuk EG, Laning ML, Foley J, et al. Spore formation and toxin production in *Clostridium difficile* biofilms. PLoS One 2014;9:e87757.
45. Schmidt NW, Wong GCL. Antimicrobial peptides and induced membrane curvature: geometry, coordination chemistry, and molecular engineering. Curr Opin Solid State Mater Sci 2013;17:151–163.
46. Lee EY, Takahashi T, Curk T, et al. Crystallinity of double-stranded RNA-antimicrobial peptide complexes modulates Toll-like receptor 3-mediated inflammation. ACS Nano 2017;11:12145–12155.
47. Lee EY, Zhang C, Di Domizio J, et al. Helical antimicrobial peptides assemble into protofibril scaffolds that present ordered dsDNA to TLR9. Nat Commun 2019;10:1012.
48. Winter SE, Thiennimitr P, Winter MG, et al. Gut inflammation provides a respiratory electron acceptor for Salmonella. Nature 2010;467:426–429.
49. Ng KM, Ferreyra JA, Higginbottom SK, et al. Microbiota-liberated host sugars facilitate post-antibiotic expansion of enteric pathogens. Nature 2013;502:96–99.
50. Park B, Buti L, Lee S, et al. Granulin is a soluble cofactor for Toll-like receptor 9 signaling. Immunity 2011;34:505–513.
51. Savidge TC, Urvil P, Oezguen N, et al. Host S-nitrosylation inhibits clostridial small molecule-activated glucosylating toxins. Nat Med 2011;17:1136–1141.
52. Biancheri P, Di Sabatino A, Corazza GR, et al. Proteases and the gut barrier. Cell Tissue Res 2013;351:269–280.
53. Antalis TM, Shea-Donohue T, Vogel SN, et al. Mechanisms of disease: protease functions in intestinal mucosal pathobiology. Nat Clin Pract Gastroenterol Hepatol 2007;4:393–402.

Author names in bold designate shared co-first authorship.

Received April 22, 2020. Accepted August 18, 2020.

Correspondence
Address correspondence to: Xinhua Chen, PhD, Division of Gastroenterology, Beth Israel Deaconess Medical Center, Harvard Medical School, 330 Brookline Avenue, Boston, Massachusetts 02215. e-mail: xchen1@bidmc.harvard.edu; fax: 617-667-2767; or Gerard C. L. Wong, PhD, Department of Bioengineering, Department of Chemistry and Biochemistry, California Nano Systems Institute, University of California, Los Angeles, 570 Westwood Plaza, Building 114, Mail Code 722710, Los Angeles, California 90095. e-mail: gclwong@seas.ucla.edu; fax: 310-794-5956.

Acknowledgments
The authors would like to thank Dr Alexander Dalpke from University of Heidelberg for his generous gifts of TLR9 mutant constructs. Author contributions: Xinhua Chen, Xiaotong Yang, Jaime de Anda, Gerard C. L. Wong, and Ciarán P. Kelly are involved study concept and design; acquisition of data; analysis and interpretation of data; drafting of the manuscript; Ciarán P. Kelly, Gerard C. L. Wong, and Xinhua Chen obtained funding and provided study supervision; Kelsey S. Shields, Joshua Hansen, Ishan J. Patel, Hua Xu, Eric U. Yee, Joshua Hansen, Hua Xu provided technical support. Marianne A. Grant, Mária Džunková, Dan Li, and Jaime de Anda were involved in acquisition of data. Douglas T. Golenbock provided material support and study design.

Conflicts of interest
The authors disclose no conflicts.

Funding
This work was supported by Irving W. and Charlotte F. Rabb Award (to Xinhua Chen), Crohn's and Colitis Foundation of America (to Xinhua Chen), Young Investigator Award for Probiotic Research (to Xinhua Chen), National Institutes of Health (NIH) National Institute of Allergy and Infectious Diseases RO1 AI095256, RO1 AI116596 (to Ciarán P. Kelly), NIH RO1 AI143730, NIH RO1 AI052453, National Science Foundation (NSF) DMR1808459 (to Gerard C. L. Wong), NSF Graduate Research Fellowship Program DGE-1650604 (to Jaime de Anda). Use of the Stanford Synchrotron Radiation Lightsource, SLAC National Accelerator Laboratory, is supported by the U.S. Department of Energy, Office of Science, Office of Basic Energy Sciences under contract no. DE-AC02-76SF00515. The Stanford Synchrotron Radiation Lightsource Structural Molecular Biology Program is supported by the U.S. Department of Energy, Office of Biological and Environmental Research, and by the NIH, National Institute of General Medical Sciences (including P41GM103393).

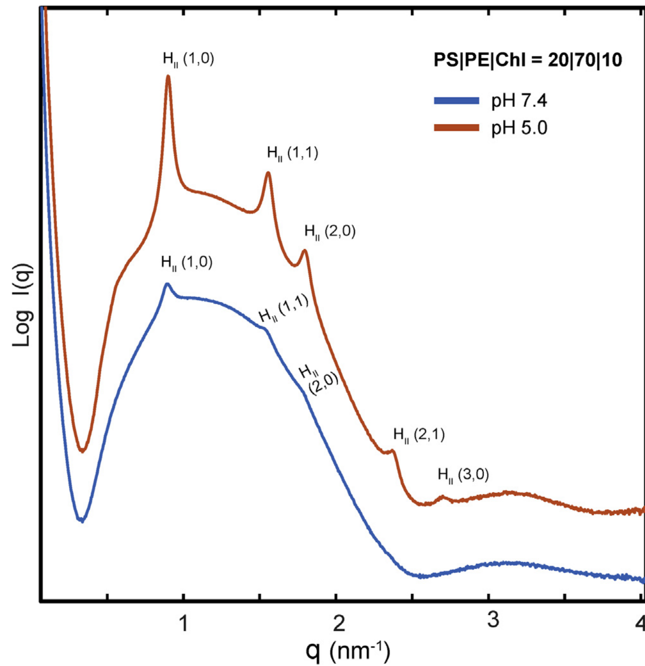

Supplementary Figure 1. Only hexagonal phases were present for the model membrane SUVs suspensions. SAXS spectra from 20/70/10 phosphatidylserine (PS)/phosphatidylethanolamine (PE)/cholesterol (Chl) model membrane suspensions only presented hexagonal Bragg peaks as annotated on the curves. The corresponding periodicity for these phases is 8.1 nm at pH 5, and 8.2 nm at pH 7.4.

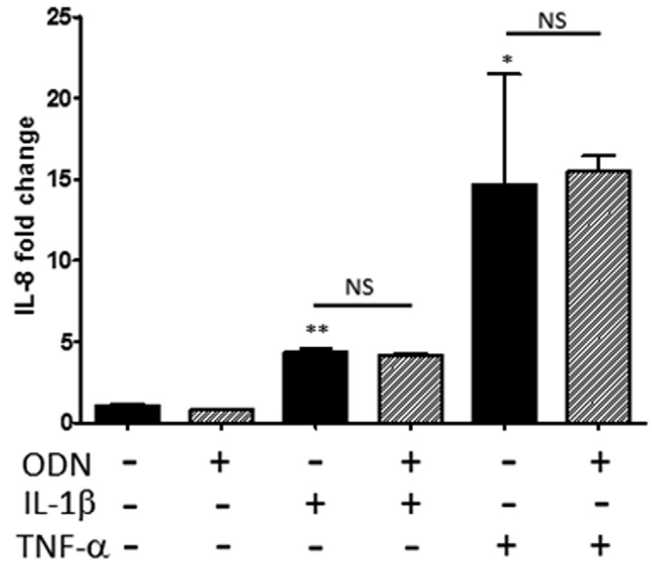

Supplementary Figure 3. TLR9 Antagonist ODN TTAGGG attenuates TcdA-induced IL-8 production in HT29 cells. Human colonic epithelial HT-29 cells were treated with medium as a control (ctrl), 25μM ODN TTAGGG (ODN), TcdA (100nM) or TcdA together with ODN (TcdA+ODN) for 14 hours. IL-8 production was measured by ELISA and normalized into fold change. * denotes $P<.05$, *Student's t-test.*

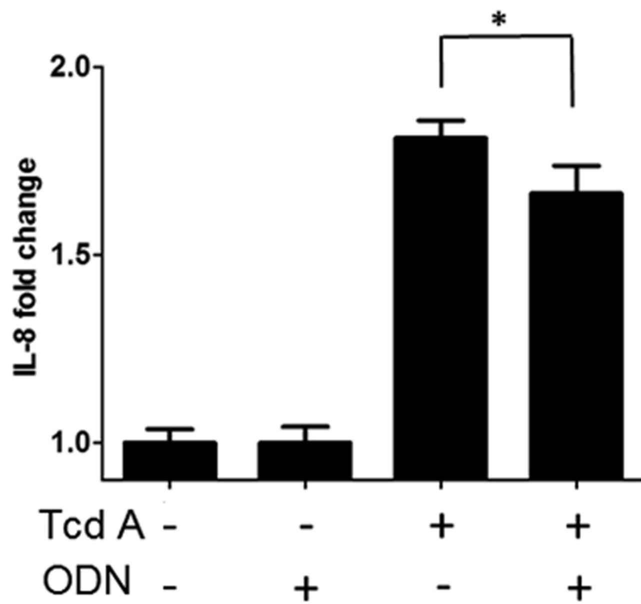

Supplementary Figure 2. TLR9 Antagonist ODN TTAGGG does not inhibit IL-8 production induced by IL-1β or TNF-a in HT29 cells. Human colonic epithelial HT-29 cells were treated with medium as control (ctrl), 25 μM ODN TTAGGG (ODN), IL-1β(1 ng/mL), TNF-a (10 ng/mL), or each cytokine in the presence of ODN (+ODN) for 14 hours. IL-8 production was measured by ELISA and normalized to fold change. ** denotes $P<.01$ compared to medium control; *denotes $P<.05$ compared to medium control; NS denotes $p>0.05$ and statistically non-significant, *Student's t-test.*